



Effects of solvent polarity and solvent viscosity on the fluorescent properties of molecular rotors and related probes

M.A. Haidekker^{a,*}, T.P. Brady^b, D. Lichlyter^a, E.A. Theodorakis^b

^a Department of Biological Engineering, University of Missouri-Columbia, Columbia, MO 65211, USA

^b Department of Chemistry and Biochemistry, University of California San Diego, La Jolla, CA 92093, USA

Received 17 May 2005

Available online 22 September 2005

Abstract

Fluorescent molecular rotors belong to a group of twisted intramolecular charge transfer complexes (TICT) whose photophysical characteristics depend on their environment. In this study, the influence of solvent polarity and viscosity on several representative TICT compounds (three Coumarin derivatives, 4,4-dimethylaminobenzonitrile DMABN, 9-(dicyanovinyl)-julolidine DCVJ), was examined. While solvent polarity caused a bathochromic shift of peak emission in all compounds, this shift was lowest in the case of molecular rotors. Peak intensity was influenced strongly by solvent viscosity in DMABN and the molecular rotors, but polarity and viscosity influences cannot be separated with DMABN. Coumarins, on the other hand, did not show viscosity sensitivity. This study shows the unique suitability of molecular rotors as fluorescent viscosity sensors.

© 2005 Elsevier Inc. All rights reserved.

Keywords: Viscosity; Biofluids; TICT; Molecular rotors

1. Introduction

Many cellular and organismal functions are linked to the viscosity of their environment, and several diseases are known to be accompanied by changes in viscosity. For example,

* Corresponding author. Fax: +1 573 884 5650.

E-mail address: HaidekkerM@missouri.edu (M.A. Haidekker).

alterations in cell membrane viscosity have been linked to atherosclerosis [1], cell malignancy [2], hypercholesterolemia [3], and diabetes [4,5]. The role of cytoplasmic viscosity has received comparatively little attention, although changed cytoplasmic viscosity is suspected to be involved in, for example, smoking and lung macrophage activation [6,7]. On a more macroscopic scale, viscosity changes in blood plasma [8–10] as well as lymphatic fluid [11,12] have been linked to various disease states. In-depth investigation of viscosity, particularly rapid viscosity changes on a microscopic scale, requires the availability of new measurement methods. Conventional mechanical viscometers are cumbersome to use and are incapable to perform real-time viscosity measurements.

The precise measurements of viscosity in biological systems, and in particular real-time measurements of viscosity changes on a microscopic scale, require the development of methods that are applicable at the molecular level. Some success with such an approach has been accomplished through the use of molecular rotors. These are fluorescent molecules with a viscosity-dependent quantum yield. Molecular rotors have been successfully applied as microviscosity probes in polymerization processes [13], phospholipid bilayers [14,15], as well as a cell membrane viscosity probe [16]. Particularly for the use in the cell membrane, special lipophilic molecular rotors were introduced [17,18]. Molecular rotors have also been used to probe reorganization processes in the cytoskeleton [19,20], and they have been bound to bioactive substances, such as actin [21], calmodulin [22], and IgG [23]. Clearly, molecular rotors have shown great potential as fluorescent probes in biological studies [24].

From the standpoint of chemical structure, molecular rotors belong to a group of fluorescent dyes that form twisted intramolecular charge transfer complexes (TICT) [25]. In TICT molecules, an electron donor (often a nitrogen atom attached to a π -system) and an electron acceptor unit (frequently a nitrile group) are coupled through a motif of alternating single and double bonds. The two units can rotate relative to each other. After photon absorption, in the excited-state, this rotation or twisting motion alters the fluorescence emission characteristics. A well-explored example for a TICT molecule is 4,4-dimethylaminobenzonitrile (DMABN) [26]. It is known in polar solvents to move from its local excited (LE) state into a TICT state by twisting around a single bond. Deexcitation from the TICT state occurs at a lower energy level, leading to a red-shifted second emission peak. In contrast, molecular rotors deexcite nonradiatively from the TICT state [27]; therefore, they do not show dual emission peaks. However, TICT formation rate decreases with increasing microviscosity of the environment [28], so that the emission intensity is increased in viscous solvents [29].

Although several fluorescent molecules are known to form TICT states [30–32], molecular rotors appear to show unique properties as viscosity probes. In an effort to elucidate this profile and clarify the difference in probe sensitivity toward solvent polarity and viscosity, we tested representative members of different TICT classes and compared their photophysical behavior in solvents of varying polarity and viscosity.

2. Materials and methods

2.1. Preparation of fluorescent probes

The structures of the fluorophores examined in this study are shown in Fig. 1. ((7-Amino-4-methylcoumarin-3-acetyl) amino) hexanoic acid (AMCA), Coumarin 1, and

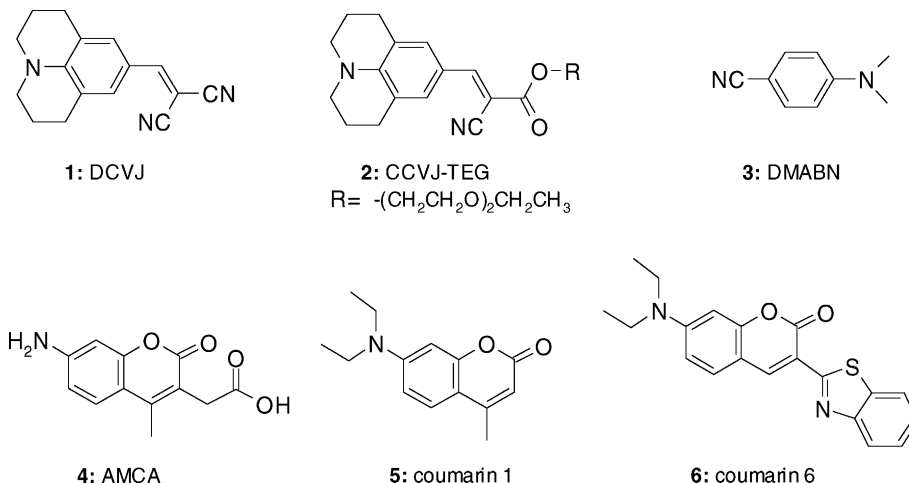


Fig. 1. Structures of the dyes examined. **1** and **2** belong to the group referred to as molecular rotors, **3** is dimethyl amino benzo nitrile, and **4–6** are Coumarin derivatives.

Coumarin 6 were purchased from Pierce, Rockford, IL and Acros Organics (Fisher), Pittsburgh, PA. 9-(Dicyanovinyl)-julolidine (DCVJ), 4,4-dimethylaminobenzonitrile (DMABN), and all solvents were purchased from Sigma–Aldrich.

9-(2-Cyano-2-hydroxy carbonyl)-vinyl julolidine–triethyleneglycol ester (CCVJ-TEG) was synthesized by our group [33]. Briefly, to a solution of 4-formyl julolidine (2 mmol) and β -cyanoester of triethylene glycol (2 mmol) in tetrahydrofuran (10 ml) was added DBU (2.1 mmol). After stirring for 1 h at 25 °C, the mixture was concentrated and the residue was subjected to silica gel chromatography (10–50% ether in hexanes) to afford CCVJ-TEG.

Each dye was dissolved in DMSO to create a stock solution. Then, a small volume (2–25 μl) was added to 5 ml of each solvent and examined for solubility. Dye concentrations ranged from 2.5 to 100 μM based on the expected quantum yield for each dye. The concentration was then kept constant for all solvents. Any dye–solvent combination exhibiting poor solubility was excluded from the data. Because of the hydrophobic nature of most dyes, water was not used as a solvent. The dielectric constant of the solvents was used as an index of its polarity. Viscosity and dielectric constant values were taken from [34] and are listed in Table 1.

Mixtures of ethylene glycol and glycerol were prepared by adding stock dye solution to 5 ml of ethylene glycol to obtain prestained ethylene glycol at tenfold of final concentration. 0.5 ml of prestained ethylene glycol was then mixed with 0.5 ml unstained ethylene glycol and 4 ml glycerol, with 1 ml ethylene glycol and 3.5 ml glycerol, with 1.5 ml ethylene glycol and 3 ml glycerol, with 2 ml ethylene glycol and 2.5 ml glycerol, and with 3.5 ml ethylene glycol and 1 ml glycerol to afford solutions of different viscosity and constant dye concentration. Viscosity values of the mixtures were calculated from Eq. (1) [35],

$$\ln \eta_{\text{mix}} = \sum_{i=1}^2 w_i \cdot \ln \eta_i, \quad (1)$$

Table 1
Solvent properties

Solvent	Solvent type	Dielectric constant ϵ	Viscosity η (mPa s) (20 °C)
Water	Polar protic	80.1	1
Ethylene glycol	Polar protic	37.7	13.5
Glycerol	Polar protic	42.5	945
Ethanol	Polar protic	25	1.2
Methanol	Polar protic	33.6	0.59
Dimethylsulfoxide	Dipolar aprotic	48.9	2.47
Dimethylformamide	Dipolar aprotic	38.3	0.85
Acetone	Dipolar aprotic	20.7	0.32
Methylene chloride	Nonpolar	9.14	0.44
Benzene	Nonpolar	2.27	0.65
Toluene	Nonpolar	2.39	0.59
Hexane	Nonpolar	1.89	0.31

where η_i is the viscosity of the individual constituent, and w_i is the weight component ($0 < w_i < 1$).

2.2. Fluorescent spectroscopy

After mixing for 1 h at room temperature each sample was scanned on a Fluoromax 3 spectrofluorometer (Jobin Yvon). The excitation wavelength was optimized for each solvent. Slits settings were 4 nm for DMABN and DCVJ, 2.5 nm for CCVJ-TEG, 1 nm for all three Coumarin dyes. The emission intensity in counts per second and peak emission and excitation wavelength data are recorded. Methacrylate cuvettes were used for most solvents except methanol and ethanol, where glass cuvettes were used.

3. Results

All fluorescent probes exhibited a bathochromic shift of the emission peak in polar solvents and a related increase of the Stokes shift. The excitation shift was comparably small (10 nm or less in the most extreme cases). Emission spectra of DMABN in some selected solvents are shown in Fig. 2. Partial quenching of DMABN emission as well as the red-shifted secondary peak in polar solvents can be seen, which is known to originate from TICT-state deexcitation [36]. In glycerol, the higher viscosity partially inhibits TICT formation, and deexcitation takes place predominantly from the LE state (Fig. 2). As opposed to DMABN, the Coumarins do not exhibit dual emission peaks. Representative spectra of Coumarin 1 can be seen in Fig. 3. A different behavior can be observed in Fig. 4, the corresponding emission spectra of DCVJ. While the bathochromic shift in polar solvents is less pronounced than in Coumarin 1, emission intensity in viscous solvents (ethylene glycol and glycerol) was markedly increased.

Fig. 5 shows the Stokes shift in dependency of the solvent dielectric constant. DMABN is most susceptible to solvent polarity with a slope of $m = 1.88$ ($r^2 = 0.75$), whereas changes of the Stokes shift is in the same order of magnitude in DCVJ, CCVJ-TEG, and the Coumarins (DCVJ: $m = 0.36$, $r^2 = 0.6$, CCVJ-TEG: $m = 0.18$, $r^2 = 0.35$; AMCA: $m = 0.49$, $r^2 = 0.73$; Coumarin 1: $m = 0.62$, $r^2 = 0.71$; Coumarin 6: $m = 0.39$, $r^2 = 0.2$).

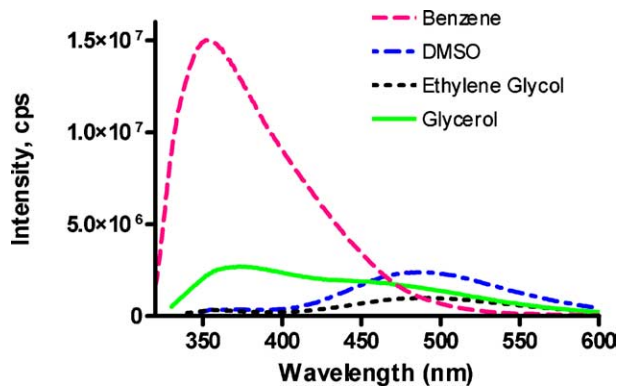


Fig. 2. Emission spectra of DMABN in selected solvents. DMABN shows the highest emission intensity in nonpolar solvents (benzene) and exhibits a secondary, red-shifted emission peak in polar solvents (e.g., DMSO and ethylene glycol). This secondary peak originates from deexcitation from the TICT state. In glycerol, the higher viscosity partially inhibits TICT formation, and deexcitation takes place predominantly from the LE state.

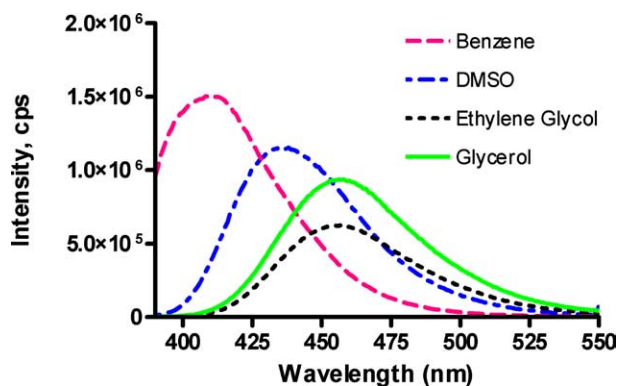


Fig. 3. Emission spectra of Coumarin 1 in selected solvents. No secondary emission peak was seen, but the emission spectra markedly shifted to the red in more polar solvents.

DMABN was the only dye to exhibit two distinct emission peaks, corresponding to the LE and TICT states. The LE peak is strongly quenched by polarity (Fig. 6). The red-shifted TICT emission peak increases in polar media of low viscosity. Therefore, not only the Stokes shift but also the emission intensity of DMABN strongly depends on the polarity of the solvent. In solvents of approximately constant polarity but with high variations of viscosity, the intensity of the LE peak increases strongly with viscosity (Fig. 7). The TICT peak also increases with viscosity but to a lesser degree. Since glycerol has a slightly higher dielectric constant than ethylene glycol, this effect can be purely attributed to viscosity.

In Fig. 8, the dependency of peak emission intensity on the viscosity of the solvent can be seen. While the Coumarin dyes exhibit only very weak dependency of their peak emission with viscosity, the molecular rotors (both DCVJ and CCVJ-TEG) show a very strong increase of emission intensity with the solvent's viscosity. With DMABN, this trend is not

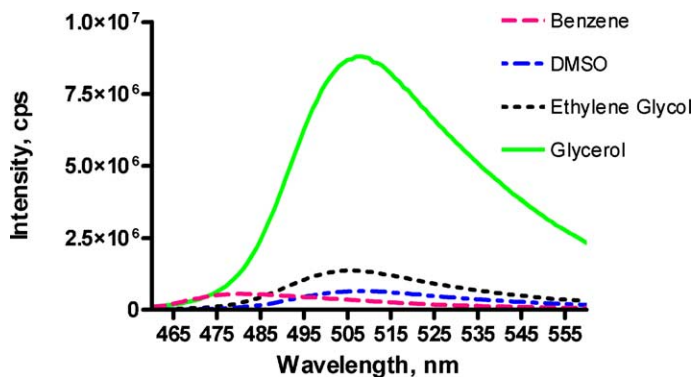


Fig. 4. Emission spectra of DCVJ in selected solvents. No secondary emission peak was seen, and the bathochromic shift in polar solvents was less pronounced than in Coumarin 1. Emission intensity increased in the moderately viscous ethylene glycol and in the highly viscous glycerol.

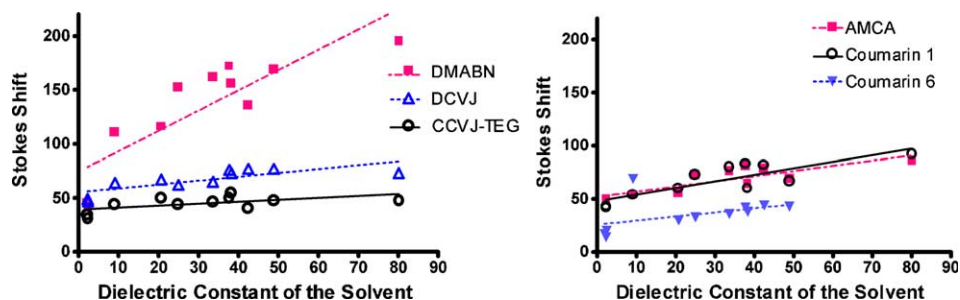


Fig. 5. Stokes shift of the different dyes in dependency of the dielectric constant of the solvents. DMABN shows the highest increase of the Stokes shift (slope $m = 1.9$, $r^2 = 0.75$). The slope is markedly lower with the molecular rotors (DCVJ: $m = 0.36$, $r^2 = 0.6$, CCVJ-TEG: $m = 0.18$, $r^2 = 0.35$) and the Coumarins (AMCA: $m = 0.49$, $r^2 = 0.73$; Coumarin 1: $m = 0.62$, $r^2 = 0.71$; Coumarin 6: $m = 0.39$, $r^2 = 0.2$).

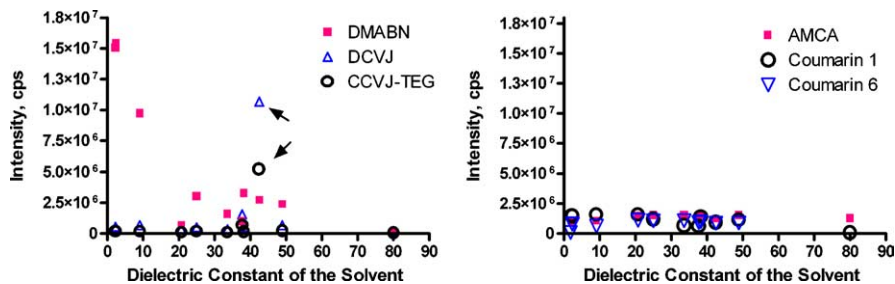


Fig. 6. Changes of peak emission intensity in different solvents. While none of the Coumarins show significant changes of emission intensity, DMABN clearly exhibits quenching when exposed to solvents of higher dielectric constant. Neither DCVJ nor CCVJ-TEG shows significant intensity changes with solvent polarity. Glycerol is the solvent for the two points indicated by arrows where the markedly increased emission intensity is caused by high-viscosity rather than polarity.

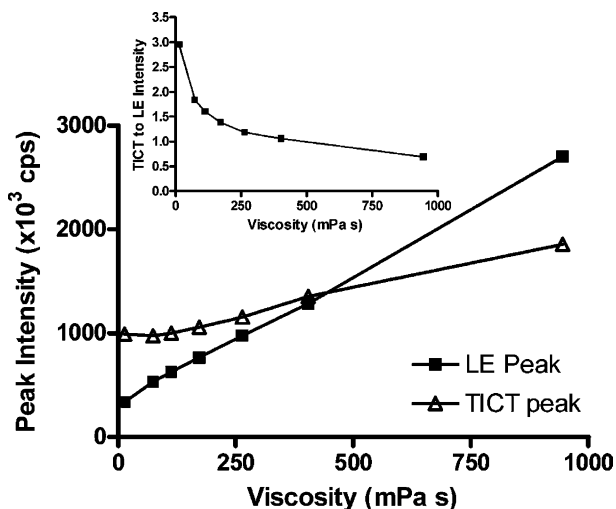


Fig. 7. Changes of DMABN peak emission intensity in solvents of different viscosity but approximately constant polarity (ethylene glycol and glycerol mixtures). Inset: Ratio of TICT peak intensity to LE peak intensity in dependency of solvent viscosity. LE peak emission strongly increases with the viscosity of the solvent, while the TICT peak shows a less strong dependency. This behavior can be explained with partial inhibition of TICT formation in high-viscosity solvents.

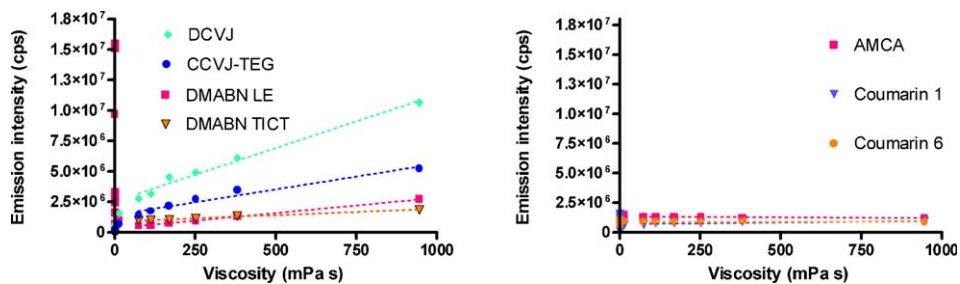


Fig. 8. Dependency of the peak emission intensity on the viscosity of the solvent. The Coumarin dyes exhibit only a very weak dependency of the peak emission on the viscosity. The molecular rotors and, to a lesser extent, DMABN, show increased peak emission with solvent viscosity. However, nonpolar solvents with low-viscosity increase DMABN emission from the LE state more than highly viscous solvents.

maintained, because of the additional influence of solvent polarity. In Fig. 8, regression lines are provided for data points originating from mixtures of ethylene glycol and glycerol. No significant correlation between viscosity and intensity was found for AMCA and Coumarin 6; For Coumarin 1, intensity increases about 264 counts per mPa s ($R^2 = 0.7$, $P = 0.04$). LE and TICT emission of DMABN increases by 2500 counts per mPa s and 1030 counts per mPa s, respectively ($R^2 > 0.99$, $P < 0.0001$). The molecular rotors show the highest viscosity-dependent intensity increase with 8800 counts per mPa s (DCVJ, $R^2 = 0.98$, $P < 0.0001$) and 4215 counts per mPa s (CCVJ-TEG, $R^2 = 0.96$, $P < 0.001$). From Fig. 8, it can be seen that the relationship between intensity and viscosity for molecular rotors is not linear. The dependency of the emission intensity of DCVJ and CCVJ-TEG can excellently be described through a power-law (Fig. 9, Eq. (2)),

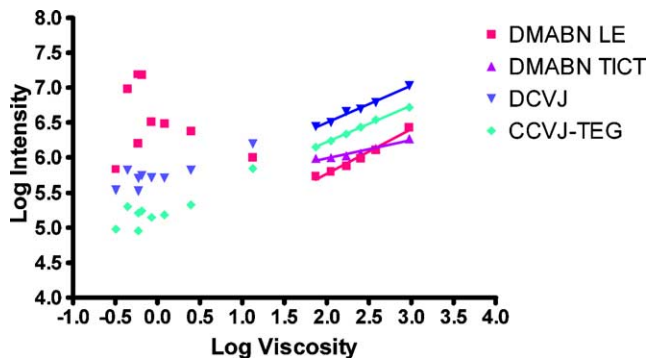


Fig. 9. Peak emission intensity and viscosity of the solvent displayed in double logarithmic scale. The slopes of the regression lines correspond to the exponent x in Eq. (2). At low viscosities, DMABN emission intensity is dominated by solvent polarity.

$$I_{\text{Peak}} = C \cdot \eta^x, \quad (2)$$

with the exponents $x = 0.40$ (DCVJ, $R^2 = 0.97$) and $x = 0.49$ (CCVJ-TEG, $R^2 = 0.98$). If polarity effects are minimized (mixtures of ethylene glycol and glycerol), the power-law relationship even better describes the intensity–viscosity relationship with $x = 0.53$ ($R^2 > 0.99$) for DCVJ and $x = 0.52$ ($R^2 > 0.99$) for CCVJ-TEG. Under this model, the LE emission of DMABN shows a similar exponent of $x = 0.64$ ($R^2 = 0.98$), while the TICT exponent is markedly lower with $x = 0.26$ ($R^2 = 0.94$).

4. Discussion

The goal of this study was to relate the photophysical properties of molecular rotors to two solvent properties: viscosity and polarity, and to compare these properties to other known TICT molecules. A wide variety of fluorophores with TICT characteristics exist [37]. One compound, DMABN, has been well described. Other TICT complexes, among them Coumarin derivatives [30] have been investigated with respect to solvent interaction. We have recently focused on a specific subclass of TICT fluorophores which are termed molecular rotors [28]. These compounds, based on the common motif of an electron-donating nitrogen (either inside a julolidine group or a substituted amino group) and electron-accepting nitrile, show a strict power-law relationship of their emission intensity with the solvent viscosity which has first been derived analytically and verified experimentally by Förster and Hoffmann [38] in a related dye.

Molecular rotors have been used as viscosity-sensitive fluorescent probes in a wide range of biological applications [13–16,19–24]. A rigid mathematical relationship between intensity and viscosity exists [38]. As a consequence, fluorescence spectroscopy can be used to determine the viscosity of biofluids, such as blood plasma [39], or aqueous starch solutions [40] with very high precision. In fact, one study has indicated that precision of conventional rheometers can be exceeded by use of molecular rotors [41]. Also, molecular rotors pose tremendous advantages in studies where the microscopic resolution of local viscosity is important, for example, in phospholipid bilayer systems [14] or in the cell membrane [16]. However, since molecular rotors show TICT behavior,

the influence of other solvent parameters, most importantly polarity, is not clear. This is an important question, because some fluorescent dyes employed as microviscosity probes are polarity-sensitive. For example, the probe Laurdan (2-dimethylamino-6-lauronaphthalene), used as cell membrane microviscosity probe [42,43], changes its properties based on water intercalation into the membrane [44], which changes the polarity of the environment. In contrast, a molecular rotor's emission intensity is based on the restricted ability to form TICT states in viscous solvents; its emission is therefore directly related to microviscosity.

The dielectric constant of a compound is an index of its polarity. Generally, polar solvent molecules reorient themselves in the proximity of a fluorescent dye after photoexcitation. As a consequence, some excited-state energy is transferred from the fluorophores to the solvent, and the emission peak shows a bathochromic shift. This effect was observed in all TICT fluorophores examined in this study, but most pronounced in DMABN (Fig. 5). In contrast, the two molecular rotors exhibit the smallest change of the Stokes shift with solvent polarity.

Although a smaller variation of the Stokes shift is favorable for viscosity-sensitive probes, it does not play a key role, because peak emission intensity is used to determine solvent viscosity. Relating emission intensity to polarity and viscosity reveals the unique position of molecular rotors. The peak emission of Coumarin dyes is almost insensitive to both polarity and viscosity of the medium (Figs. 6 and 8). Their high and constant quantum yield makes these compounds attractive as laser dyes.

DMABN has a unique position, because both its LE and TICT states allow relaxation through photon emission. In the other TICT compounds (Coumarins and molecular rotors), TICT formation leads to nonradiative deexcitation, and TICT formation is inversely related to fluorescence emission. As a consequence, only DMABN exhibits a dual emission peak, where the intensity shifts from the TICT (bathochromic) emission peak to the LE peak as solvent viscosity is increased (Fig. 7). Of all compounds tested, DMABN shows the most complex behavior. Both polarity and viscosity strongly influence emission. Finally, molecular rotors exhibit strong viscosity-dependent emission, but only minimal influence of polarity on emission intensity.

5. Conclusion

Three groups of TICT-forming molecules were tested. We found that the emission wavelength of Coumarins was influenced by solvent polarity, but neither viscosity nor polarity had a major impact on emission intensity. DMABN exhibited a complex dependency of emission intensity on both solvent polarity and viscosity, making it difficult to separate the influences of viscosity and polarity. Molecular rotors (DCVJ and its derivatives) showed highly viscosity-dependent emission intensity combined with low sensitivity towards solvent polarity. With this property, molecular rotors are ideally positioned as microviscosity probes even in environments where polarity changes are expected.

Acknowledgment

The authors gratefully acknowledge financial support through NIH Grant 1R21-RR018399.

References

- [1] G. Deliconstantinos, V. Villiotou, J.C. Stavrides, *Biochem. Pharmacol.* 49 (1995) 1589–1600.
- [2] M. Shinitzky, in: M. Shinitzky (Ed.), *Physiology of Membrane Fluidity*, CRC Press, Boca Raton, 1984, pp. 1–51.
- [3] M.M. Gleason, M.S. Medow, T.N. Tulenko, *Circ. Res.* 69 (1991) 216–227.
- [4] O. Nadiy, M. Shinitzky, H. Manu, D. Hecht, C.T. Roberts Jr., D. LeRoith, Y. Zick, *Biochem. J.* 298 (Pt 2) (1994) 443–450.
- [5] W. Osterode, C. Holler, F. Ulberth, *Diabet. Med.* 13 (1996) 1044–1050.
- [6] W. Moller, W. Barth, W. Pohlit, M. Rust, R. Siekmeier, W. Stahlhofen, J. Heyder, *Toxicol. Lett.* 88 (1996) 131–137.
- [7] W. Stahlhofen, W. Moller, *J. Aerosol. Med.* 5 (1992) 221–228.
- [8] J. Harkness, *Biorheology* 8 (1971) 171–193.
- [9] R.L. Letcher, S. Chien, T.G. Pickering, J.E. Sealey, J.H. Laragh, *Am. J. Med.* 70 (1981) 1195–1202.
- [10] M.A. McGrath, R. Penny, *J. Clin. Invest.* 58 (1976) 1155–1162.
- [11] D.O. Bates, J.R. Levick, P.S. Mortimer, *Clin. Sci. (Lond.)* 85 (1993) 737–746.
- [12] H. Schad, H. Brechtelsbauer, *Z. Lymphol.* 10 (1986) 14–19.
- [13] R.O. Loutfy, *Pure Appl. Chem.* 58 (1986) 1239–1248.
- [14] C.E. Kung, J.K. Reed, *Biochemistry* 25 (1986) 6114–6121.
- [15] S. Lukac, *J. Am. Chem. Soc.* 106 (1984) 4386–4392.
- [16] M.A. Haidekker, N. L'Heureux, J.A. Frangos, *Am. J. Physiol. Heart Circ. Physiol.* 278 (2000) H1401–H1406.
- [17] M. Haidekker, T. Brady, K. Wen, C. Okada, H. Stevens, J. Snell, J. Frangos, E. Theodorakis, *Bioorg. Med. Chem.* 10 (2002) 3627–3636.
- [18] M.A. Haidekker, T. Ling, M. Anglo, H.Y. Stevens, J.A. Frangos, E.A. Theodorakis, *Chem. Biol.* 8 (2001) 123–131.
- [19] C.E. Kung, J.K. Reed, *Biochemistry* 28 (1989) 6678–6686.
- [20] T. Furuno, R. Isoda, K. Inagaki, T. Iwaki, M. Noji, M. Nakanishi, *Immunol. Lett.* 33 (1992) 285–288.
- [21] T. Iio, S. Takahashi, S. Sawada, *J. Biochem.* 113 (1993) 196–199.
- [22] T. Iio, M. Itakura, S. Takahashi, S. Sawada, *J. Biochem.* 109 (1991) 499–502.
- [23] T. Iwaki, C. Torigoe, M. Noji, M. Nakanishi, *Biochemistry* 32 (1993) 7589–7592.
- [24] M.L. Viriot, M.C. Carré, C. Geoffroy-Chapotot, A. Brembilla, S. Muller, J.-F. Stoltz, *Clin. Hemorheol. Microcirc.* 19 (1998) 151–160.
- [25] W. Rettig, R. Lapouyade, in: J.R. Lakowicz (Ed.), *Topics in Fluorescence Spectroscopy, Probe Design and Chemical Sensing*, vol. 4, Plenum Press, New York, 1994, pp. 109–149.
- [26] K. Rotkiewicz, K.H. Grellmann, Z.R. Grabowski, *Chem. Phys. Lett.* 19 (1973) 315–318.
- [27] M.S.A. Abdel-Mottaleb, R.O. Loutfy, R. Lapouyade, *Photochem. Photobiol.* 48 (1989) 87–93.
- [28] R.O. Loutfy, B.A. Arnold, *J. Phys. Chem.* 86 (1982) 4205–4211.
- [29] K.Y. Law, *Chem. Phys. Lett.* 75 (1980) 545–549.
- [30] S. Senthilkumar, S. Nath, H. Pal, *Photochem. Photobiol.* 80 (2004) 104–111.
- [31] G. Jones, J.A. Jimenez, *J. Photochem. Photobiol. B* 65 (2001) 5–12.
- [32] C. Vijila, A. Ramalingam, P.K. Palanisamy, V. Masilamani, *Spectrochim. Acta A. Mol. Biomol. Spectrosc.* 57 (2001) 491–497.
- [33] M.A. Haidekker, T.P. Brady, S.H. Chalian, W. Akers, D. Lichlyter, E.A. Theodorakis, *Bioorg. Chem.* 32 (2004) 274–289.
- [34] J.A. Dean, *Lange's Handbook of Chemistry*, McGraw-Hill, New York, 1992.
- [35] R.H. Perry, D.W. Green, J.O. Maloney, *Perry's Chemical Engineer's Handbook*, McGraw-Hill, New York, 1984.
- [36] Z.G. Grabowski, K. Rotkiewicz, A. Siemiarz, D.J. Cowley, W. Baumann, *Nouv. J. Chim.* 3 (1979) 443–454.
- [37] M. Kasha, *Basic Life Sci.* 58 (1991) 231–251.
- [38] Th. Förster, G. Hoffmann, *Z. Phys. Chem.* 75 (1971) 63–76.
- [39] M.A. Haidekker, A.G. Tsai, T. Brady, H.Y. Stevens, J.A. Frangos, E. Theodorakis, M. Intaglietta, *Am. J. Physiol. Heart Circ. Physiol.* 282 (2002) H1609–H1614.
- [40] W. Akers, M.A. Haidekker, *J. Biomech. Eng.* 126 (2004) 340–345.
- [41] W. Akers, M.A. Haidekker, *J. Biomech. Eng.* 127 (2005) 450–454.

- [42] T. Parasassi, M. Di Stefano, M. Loiero, G. Ravagnan, E. Gratton, *Biophys. J.* 66 (1994) 120–132.
- [43] T. Parasassi, M. Di Stefano, G. Ravagnan, O. Sapora, E. Gratton, *Exp. Cell Res.* 202 (1992) 432–439.
- [44] T. Parasassi, M. Di Stefano, M. Loiero, G. Ravagnan, E. Gratton, *Biophys. J.* 66 (1994) 763–768.